IEEE Access
Multidisciplinary | Rapid Review | Open Access Journal

Received November 16, 2018, accepted November 27, 2018, date of publication December 6, 2018,
date of current version January 7, 2019.

Digital Object Identifier 10.1109/ACCESS.2018.2885402

Sensitivity of Low-Voltage Variable-Frequency Devices to Voltage Sags

YONGHAI XU[1], (Member, IEEE), WENQING LU[1], (Student Member, IEEE), KUN WANG[1], CHENYI LI[2], AND WASEEM ASLAM[1]

[1]State Key Laboratory of Alternate Electrical Power System With Renewable Energy Sources, North China Electric Power University, Beijing 102206, China
[2]State Grid Sichuan Electric Power Corporation Chengdu Power Supply Company, Chengdu 610011, China

Corresponding author: Wenqing Lu (daqing1033@163.com)

This work was supported by the National Natural Science Foundation of China under Grant 51277069.

ABSTRACT Variable frequency drives (VFDs) are the types of power electronic device commonly used to drive motors with a wide range of industrial and practical applications, especially in power systems. VFDs are sensitive to voltage sag, thereby limiting their application. However, the difficulty in determining the detailed voltage sag tolerance characteristics of VFDs is due to various influencing factors, and the tolerance curve obtained from test results is updated as mainstream low-voltage VFDs change. This paper is the first to perform an in-depth analysis on the influence and operation mechanism of voltage sags on VFDs. Voltage sag types, which are regarded as the important influencing factors, are explored for their different impacts on VFDs from the perspective of energy. Then, eight commonly used low-voltage VFDs with small and medium powers (7.5 and 18.5 kW) are selected as the test objects. The influence of voltage sags on VFDs is tested, and the equipment parameters (protection modes and control modes of VFDs, and load torque and speed) and voltage sag characteristics factors (sag types, voltage magnitude before voltage sag, and harmonics) are considered. Finally, the general tolerance curves of the low-voltage VFDs under different sag types are extracted via comprehensive analyses and processing of more than 13 000 sets of test data. Based on the test data, this paper further explores the influence of voltage sag on the motor by using the permanent magnet synchronous motor (PMSM) as an example, which is used as the load during the tolerance test. Operation performance of the PMSM driven by different VFDs is also discussed.

INDEX TERMS Variable frequency drive, voltage sag, tolerance curve, PMSM.

I. INTRODUCTION

Variable-frequency Drive (VFD) is a typical equipment frequently applied in power systems and various industrial and practical fields. These devices are sensitive to voltage sags. When a voltage sag occurs in a power grid, VFDs may trip and cease operation, which may result in the interruption of an entire production process and cause huge economic losses. Voltage sags can also lead to the main fuel trip of a generator unit and further influence the faulted power grid once the auxiliary VFDs in a power plant faults and trips, thereby remarkably affecting the stability of the power grid [1]. Therefore, assessing the voltage sag tolerance capability of VFDs is necessary to propose practical suppression suggestions for power systems, enterprises, and users.

Limited researches have been conducted on trip curves for power electronic devices, such as VFDs, due to their complexity and high cost [2]. Reference [3] presents a methodology for predicting the number of equipment outages due to voltage sags based on the tolerance curve of equipment. However, the targeted equipment curve is not available. Many VFD and voltage sag factors must be considered, and a number of current mainstream VFDs must also be tested to practically obtain the general tolerance curve of VFDs. The main influencing factors are low-voltage protection, over-current protection, load torque and speed, and sag types [4], [5]. Reference [6] shows the mechanism of VFDs in detail and provides the test results of voltage sag tolerance capability. Reference [7] analyzes the influence of voltage magnitude before voltage sag, harmonics, a shape of voltage sag, point-on-wave and phase shift on the tolerance capability. Reference [8] studies the tolerance curve of commonly used VFDs in Canada with a voltage level of 600V but presents only the waveforms of DC voltage, motor speed and torque for a certain voltage sag. In Reference [9], voltage sag tolerance characteristics of ASDs and VFDs are studied in a simple industrial process, where only a few factors are considered.

Based on the references mentioned, the voltage sag tolerance curve was not applicable to current mainstream VFDs and limited influencing factors were considered.

Universal standard voltage tolerance curves include ITIC (Information Technology Industry Council) curve that formerly known as CBMEB (Computer & Business Equipment Manufacturers Association) for information and technology industry, SEMI (Semiconductor Equipment Materials International) F47 curve for the semiconductor industry, and voltage tolerance curves for five types of voltage sags proposed by the CIGRE/CIRED/UIE joint working group C4.110 [10]. Anyone of the curves mentioned can describe the voltage tolerance capability of arbitrary sensitive equipment roughly, such as VFDs, but lacks of accuracy. The upper and lower envelopes and the average limit shown in IEEE Std 1346-1998 [11] indicate the voltage tolerance curve standard of VFDs. However, the influence of sag types is not considered in this standard.

The motor is the main type of load driven by VFDs in practical production processes. Even if the driving VFDs could withstand voltage sag occurrences, the torque and speed of the motor would still be affected. So there may be a fault for the motor in applications where precise control is required. Studies have investigated the influence of voltage sags on the motor. Reference [12] shows that voltage sags and interruptions exceeding a certain threshold would cause PMSM to lose synchronous speed and create enlarged stator current and motor torque. Reference [13] focus on the influence of asymmetric voltage sags on the peaks of current and motor speeds. However, the studies mentioned above did not discuss the difference of the voltage sags' influence on the motor driven by VFDs. Therefore, further research on the influence of voltage sags on motors is still necessary.

Therefore, this study considers the comprehensive factors, making it possible to obtain a general voltage tolerance curve for low-voltage VFDs with small and medium power levels. First, this study analyzes the operation mechanism of VFDs and discusses the possible influencing factors of voltage sags on VFDs. Especially, voltage sag types are first taken into consideration to be an important influencing factor for tolerance capability of VFDs. Eight low-voltage VFDs with two types of powers (18.5 kW and 7.5 kW) are chosen for voltage sag tolerance tests. Considering the influencing factors of equipment and voltage sag characteristics, this study extracts different tolerance curves through comprehensive analysis and management of 13,000 sets of data. The influence of voltage sags on the motor is also investigated. PMSM is used as an example to explore the influence of voltage sags on the motor under different VFDs through analysis of the mechanism and test data.

II. MECHANISM OF VFDS AFFECTED BY VOLTAGE SAGS

A. OPERATION PRINCIPLES OF VFDS

As shown in Fig. 1, VFDs are composed of a rectifier, DC voltage stabilizer, inverter, and control loop unit. The rectifier

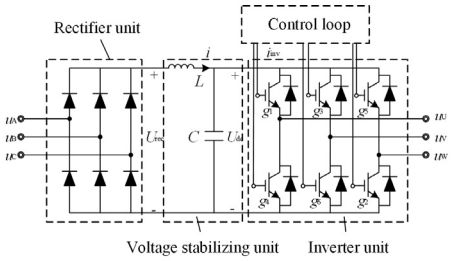

FIGURE 1. Topology of commonly used low voltage VFDs.

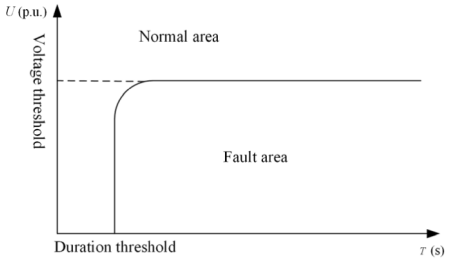

FIGURE 2. Sketch map of voltage tolerance curve of VFDs.

unit is generally a three-phase uncontrollable bridge rectifier for VFDs with small and medium power levels. The three-phase AC voltage is input into VFDs and converted to DC voltage by the rectifier unit. Energy is stored in the DC capacitor, and then the DC voltage is converted into AC voltage through the inverter circuit. The motor speed can be adjusted by controlling the switching frequency of the fully controlled devices of the inverter circuit [1].

B. INFLUENCING FACTORS ANALYSIS ON VOLTAGE SAG TOLERANCE CHARACTERISTICS OF VFDS

The voltage sag tolerance curve of VFDs is generally rectangular in shape. The curve consists of horizontal edges depending on its voltage threshold, vertical edges depending on duration threshold, and the transitional parts, as shown in Fig. 2. A voltage sag or power interruption whose duration is less than the critical duration will not cause the VFDs to malfunction. Similarly, a voltage sag, whose voltage magnitude is higher than the critical level will not cause the VFDs to trip. Thus, the normal operation area is where the duration is less than the critical duration or where the voltage magnitude is higher than the critical level, and the remaining area is called the fault area. The voltage sag tolerance curve of VFDs may differ due to various influencing factors. The parameters can be divided into two categories of equipment parameters (protection modes, control modes, and load torque and speed) and voltage sag characteristics (sag types, voltage magnitude before voltage sag, and harmonics). This study focuses on analyzing the influencing factors that remarkably affect the voltage sag tolerance characteristics of VFDs.

1) LOW-VOLTAGE AND OVER-CURRENT PROTECTION THRESHOLDS

Generally, VFDs have the DC bus for low-voltage protection and over-current protection to prevent abnormal operation or overload. When a voltage sag occurs, the AC voltage of

the input terminal reduces suddenly to mitigate the energy entering VFDs, whereas load power of the output terminal does not change. Thus, the power between the input and output terminals becomes imbalanced. The capacitor on the DC side of VFDs must discharge to regain balance, thereby reducing the voltage on the DC side of VFDs. Therefore, the DC bus voltage is lower than that of the protection threshold, and the low-voltage protection works and the VFDs trip. Instead of low-voltage protection, voltage sag may trigger over-current protection if the duration of the sag is too short. The reasons are that the load power remains unchanged and the input current increases due to the lower input voltage during the voltage sag, and the capacitor is charged by the recover input voltage and may cause an over-current after the voltage sag. The low-voltage protection and over-current protection thresholds directly determine the voltage sag tolerance capability of VFDs. The researches show that the critical duration is mainly determined by the low-voltage protection, and the critical voltage magnitude is mainly determined by the over-current protection. Sometimes the two thresholds may also be determined only by a certain one of the two protections [6], [7], [14].

When the duration of a voltage sag is less than the critical duration, the DC voltage of VFDs will recover before reducing to the threshold of low-voltage protection. Thus, the protection is not triggered. Critical duration is the responding trip time when the voltage sag magnitude is exactly equal to protection threshold. Assuming that the load power is invariant and the VFDs can withstand the voltage sag, the tolerant duration of voltage sag whose corresponding voltage magnitude is $V_{\min}$ can be inferred according to principle of energy conservation, as shown in (1) [6].

$$t = \frac{C}{2P_L}(V_0^2 - V_{\min}^2) \tag{1}$$

where: V_0 is the DC bus voltage before voltage sag; P_{L} is the load power; C is the capacitance on DC side.

Equation (1) presents that a decreased low-voltage protection threshold results in an enlarged critical duration when the capacitance and load power are constant. At the same time, a decreased voltage sag magnitude which the VFDs can withstand means their tolerance capability is enhanced.

The more the DC voltage reduces during voltage sag, the bigger the voltage variation on DC side at the moment when the supply voltage recovers, so the charge current is larger. The peak of charge current is as shown in (2) according to theoretical derivation [15].

$$\Delta i_{\max} = \sqrt{\frac{C}{L}}\Delta V_{dc} \tag{2}$$

where: L is the inductance of smoothing reactor, and its value is usually smaller; ΔV_{dc} is voltage variation on DC side when the supply voltage recovers. According to (2), the higher the over-current protection threshold is, the lower voltage sag magnitude VFDs can withstand during the voltage sag, and so the lower the critical voltage on AC side, the stronger the voltage sag tolerance capability of VFDs is.

2) LOAD TORQUE AND SPEED

The main reason why voltage on DC side reduces when the voltage sag happens is that energy of DC bus is consumed by the load. Most loads behind VFDs are motors, and the relationship between motor torque, speed and power is shown as (3) [15]:

$$P = \frac{T \cdot n}{9550} \tag{3}$$

where: T is motor torque; n is motor speed; P is motor power.

Equation (3) shows that an enlarged load torque or speed will result in an enlarged load power. The load power determines the decline rate of DC voltage when the capacitance is constant, and a large load power will result in an increased reducing rate of voltage on the DC side. Equation (1) states that an increased load power results in a decreased critical duration of the VFD's voltage sag tolerance curve. Therefore, enlarged load torque and speed will cause a weaker voltage sag tolerance capability for the VFD.

In addition, it is found in the tests that the voltage sag has different effects on the operating characteristics of the PMSM under different VFDs. It will be discussed further in Section V.

3) VOLTAGE SAG TYPES

Voltage sag type has considerable influence on the voltage sag tolerance characteristics of VFDs. Most voltage sags are caused by different short-circuit faults in the power system, which are mainly divided into three-phase, two-phase, and single-phase voltage sags after being transmitted by transformers and lines. Different types of voltage sags have different sag phases and voltage magnitudes, thus causing different average voltages on the DC bus of VFDs and tolerance characteristics of VFDs under low-voltage protection. Therefore, the voltage sag tolerance capability of VFDs can be analyzed according to magnitude of voltage on DC side under different types of voltage sags. But in fact, voltage sag type was not analyzed or taken into consideration when carrying out tolerance tests before. This paper carries out the studies on DC voltage on rectifier side to explain the difference of voltage sag tolerance characteristics of VFDs under different types of voltage sags.

According to the rectifier topology of VFDs, the capacitor is charged by the maximum one of the three line voltage (u_{AB}, u_{BC} or u_{CA}) at any moment when the power supply is normal. The average of DC voltage fluctuates between the average of the line voltage upper envelope and the peak of line voltage and keeps in a relative balance level. The DC voltage of VFDs is the peak of line voltage when the rectified current is discontinuous with a no-load run, while it is the average of the line voltage upper envelope when the rectified current is continuous. Once the voltage sag occurs, the voltage on DC side is higher than the peak of line voltage, and the DC voltage drops. When the voltage is lower than the peak line voltage, the AC line voltage starts to charge for the capacitor, and a new balance is obtained. Accordingly, the average of

the DC voltage is determined by the line voltage during the voltage sag. The voltage sag types for test recommended in IEEE P1668 are Type III (three-phase voltage sag), Type II (two-phase voltage sag), and Type I (single-phase voltage sag), and the phase voltages of different type sags are shown in (4) - (6) [16].

$$\begin{aligned}\dot{V}_a &= X \\ \dot{V}_b &= -\frac{1}{2}E - \frac{1}{2}jE\sqrt{3} \\ \dot{V}_c &= -\frac{1}{2}E + \frac{1}{2}jE\sqrt{3}\end{aligned} \tag{4}$$

$$\begin{aligned}\dot{V}_a &= E \\ \dot{V}_b &= -\frac{1}{2}E - \frac{1}{2}jV\sqrt{3} \\ \dot{V}_c &= -\frac{1}{2}E + \frac{1}{2}jV\sqrt{3}\end{aligned} \tag{5}$$

$$\begin{aligned}\dot{V}_a &= U \\ \dot{V}_b &= -\frac{1}{2}U - \frac{1}{2}jU\sqrt{3} \\ \dot{V}_c &= -\frac{1}{2}U + \frac{1}{2}jU\sqrt{3}\end{aligned} \tag{6}$$

where: E is the rated voltage; X is phase voltage of Type I voltage sag; V is phase voltage of Type II voltage sag; U is phase voltage of Type III voltage sag.

According to the phase voltages, instantaneous values of line voltages u_{AB}, u_{BC}, and u_{CA} can be computed according to phase voltage equations, which are shown in (7) - (9).

$$\begin{aligned}u_{ab} &= K_1 \sin(\omega t - \varphi_1) \\ u_{bc} &= \sqrt{6}E \sin(\omega t + \frac{\pi}{2}) \\ u_{ca} &= K_1 \sin(\omega t + \varphi_1 - \pi)\end{aligned} \tag{7}$$

$$\begin{aligned}u_{ab} &= K_2 \sin(\omega t - \varphi_2) \\ u_{bc} &= \sqrt{6}V \sin(\omega t + \frac{\pi}{2}) \\ u_{ca} &= K_2 \sin(\omega t + \varphi_2 - \pi)\end{aligned} \tag{8}$$

$$\begin{aligned}u_{ab} &= \sqrt{6}U \sin(\omega t - \frac{\pi}{6}) \\ u_{bc} &= \sqrt{6}U \sin(\omega t + \frac{\pi}{2}) \\ u_{ca} &= \sqrt{6}U \sin(\omega t - \frac{5\pi}{6})\end{aligned} \tag{9}$$

where: $K_1 = \sqrt{2(X+E/2)^2+3E^2/2}$; $K_2 = \sqrt{9E^2/2+3V^2/2}$; $\varphi_1 = \arctan\left[\sqrt{3}E/(2X+E)\right]$; $\varphi_2 = \arctan\ (V/(\sqrt{3}E))$.

Based on the above analysis, when the rectified current is continuous, the DC voltage U_{d1}, U_{d2}, and U_{d3} of VFDs for Type I, Type II, and Type III voltage sag is the average of line voltages and can be inferred respectively as shown in (10) - (12).

$$U_{d1} = \frac{\sqrt{6}}{\pi}E\sin\theta_1 + \frac{K_1}{\pi}\cos\varphi_1 + \frac{K_1}{\pi}\cos(\theta_1 - \varphi_1) \tag{10}$$

$$U_{d2} = \frac{\sqrt{6}}{\pi}V\sin\theta_2 + \frac{K_2}{\pi}\cos\varphi_2 + \frac{K_2}{\pi}\cos(\theta_2 - \varphi_2) \tag{11}$$

$$U_{d3} = \frac{3\sqrt{6}}{\pi}U \tag{12}$$

where: $\theta_1 = \arctan\left[(K_1\sin\varphi_1 + \sqrt{6}E)/(K_1\cos\varphi_1)\right]$; $\theta_2 = \arctan\left[(K_2\sin\varphi_2 + \sqrt{6}V)/(K_2\cos\varphi_2)\right]$.

When the rectified current is discontinuous at no-load, DC voltage is related to the capacitance. Therefore, its expression is complex. Here shows the rough range of DC voltage on Type I, Type II, and Type III voltage sag with no-load run: for Type I voltage sag, $U_{d1} \in \left(K_1, \sqrt{6}\,E\right)$, for Type II voltage sag, $U_{d2} \in \left(\sqrt{6}\,V, K_2\right)$, and for Type III voltage sag, $U_{d3} = \sqrt{6}\,U$.

To better compare the DC voltages for the three types of voltage sags, set magnitudes of the sag phases of Type I, Type II, and Type III voltage sag as $0.5E$, where $X = U = 0.5E$ and $V = 0$. When the rectified current is discontinuous, compute the range of peak of line voltage to obtain the DC voltages on the three voltage types of sags during no-load run, where $U_{d1} \in (1.87E, 2.45E)$, $U_{d2} \in (0, 2.12E)$, and $U_{d3} = 1.22E$. Substitute $X = U = 0.5E$ and $V = 0$ into (10)-(12), the DC voltages can be obtained as $U_{d1} = 1.70\ E$, $U_{d2} = 1.35\ E$, and $U_{d3} = 1.17\ E$ when the rectified current is continuous on the three types of voltage sags. For Type II, the DC voltage at no-load run must be larger than that during load, and the rectified current changes from intermittent to continuous when the load increases gradually. Thus, the DC voltage at no-load run must be larger than that at continuous current, which can be expressed as $U_{d2} \in (1.35E, 2.12E)$. From the above analyses, the DC voltages of VFDs decrease in turn for Type I, Type II, and Type III voltage sags both at no-load and at load. And the probabilities that three types of voltage sags trigger the low-voltage protection increase in turn. Therefore, the tolerance capability of VFDs to withstand Type I, Type II, and Type III voltage sags also weakens.

4) CONTROL MODES

At present, the commonly used control modes of VFDs are V/f control and vector control. V/f control is the simpler way to control the output voltage of VFDs. It makes motor keep its magnetic flux constant by taking control of the ratio of voltage V to frequency f to be constant so that the motor can run under the magnetic flux saturation state and its efficiency is improved. However, the adjustment range of V/f control is limited. When a voltage sag occurs, the dynamic control performance of motor is poor, which makes it difficult to accurately and stably control the operation of the motor. Therefore, most studies believe that the VFDs under the V/f control mode are more sensitive to voltage sag than that under vector control [14].

Vector control, known as a high-performance mode, converts the three-phase stationary coordinates of the motor stator into two-phase orthogonal rotating coordinates through coordinate transformation so that the three-phase stator alternating current is equivalent to a two-phase orthogonal direct current. And the decoupling control is realized by controlling

its electromagnetic torque and the flux linkage following the control way of DC motor.

5) VOLTAGE MAGNITUDE BEFORE SAGS

In power systems, the nominal voltage of the PCC is often not 1 p.u. due to fluctuations in output of generation units and load and changes of power grid structure. Before the voltage sag occurs, the supply voltage magnitude of VFDs shall be within the allowable range, that is, 0.9 p.u.-1.1 p.u. Equation (1) shows that an increased magnitude of the supply voltage before the sag leads to an increased voltage on the DC side of VFDs and an extended duration of capacitor discharge for the protection threshold during the voltage sag. Thus, VFDs can withstand voltage sags with longer duration and lower sag magnitude on higher voltage magnitude before sag.

6) HARMONICS

There are a large number of nonlinear components such as power electronic devices in power systems. They inject harmonic current into the systems, causing harmonic distortion of the voltage at the PCC point. The harmonics will affect the natural phase-change point of the rectifier diode of VFDs so that the voltage sag tolerance characteristics of VFDs are changed. According to the regulation of national standard [17], the total harmonic distortion (THD) of the PCC point at less than 1000V voltage level shall not exceed 8% and the odd harmonic content shall not exceed 5%. Reference [7] studies the influences of harmonics at different orders and phase on VFDs' tolerance capability when THD is 20%, and finds that 5th harmonic of 0° and the 7th harmonic of 180° will weaken the sag tolerance capability of VFDs, and the 5th harmonic of 180° will strength its sag tolerance capability, and the other harmonics will not affect the sag tolerance characteristics of VFDs. However, it mainly targets VFDs in one brand and the tested objects are too few. In addition, the THD value in the actual grid is usually far less than 20%, so the conclusion may not apply to the actual situation.

III. TEST PROGRAM

A. TEST PLATFORM

During the tests, the tested VFDs are used to drive PMSM which is a back-to-back combination of the motor ($PMSM_1$) and the generator ($PMSM_2$) when it is powered, and the energy of assembly returns back to the grid by the feedback VFD. The test platform mainly contains voltage sag source, control computer, tested VFD, PMSM, feedback VFD, a torque sensor and wave recorder. The wiring diagram of the test platform is shown in Fig. 3.

There are 8 tested objects including 7 brands of low-voltage VFDs with higher market share whose rated power is 18.5 kW or 7.5 kW. The parameters of the 8 VFDs are shown in Table 1. And the parameters of PMSM are shown in Table 2.

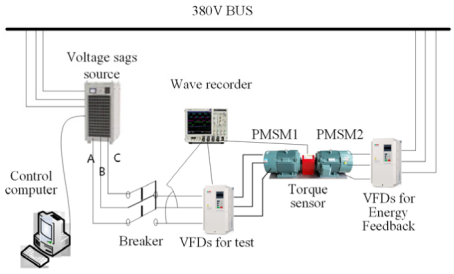

FIGURE 3. Site wiring diagram of the test platform.

TABLE 1. Parameters of the VFDs.

Variable-frequency device	Rated power	Rated voltage
VFD_1	18.5 kW	380 (-15%) - 440 V (+10%)
VFD_2	18.5 kW	380-480 V
VFD_3	18.5 kW	400V/480 V
VFD_4	18.5 kW	380 (-15%) - 480 V (+10%)
VFD_5	7.5 kW	380 V (-15%-+20%)
VFD_6	7.5 kW	380 (-15%) - 480 V (+10%)
VFD_7	7.5 kW	380 (-10%) - 440 V (+10%)
VFD_8	7.5 kW	380 V (-10%-+10%)

TABLE 2. Parameters of the tested motor.

Motor	Rated power (kW)	Rated voltage (V)	Rated current (A)	Rated Speed (rpm)
Driving motor ($PMSM_1$)	15	380	22	250
Tow motor ($PMSM_2$)	10	400	15	250

B. TEST INFLUENCING FACTORS

The test takes motor torque and speed, control modes, voltage sag types, voltage magnitude before voltage sag, and harmonics into consideration to determine how the factors affect the operation of VFDs. The parameter settings of test influence factors are shown in Table 3, and something shall be noted is as follows:

- Type III is the voltage sag type under the test factors except for voltage sag types themselves. When a certain influencing factor is tested, other factors are set to default, that is, the motor torque and speed are set to 100%, the control mode is vector control, the voltage magnitude before voltage sag is at 100%, and no harmonics are available.
- The low-voltage protection and over-current protection are not regarded as the test influencing factors because the manufacturers of some tested VFDs do not open editing functions of the two protections, which make the protection thresholds cannot be set.

TABLE 3. Parameter settings for influencing factors.

	Influencing factors	State 1	State 2	State 3	State 4
Equipment parameters	Motor torque	0% T_N	25% T_N	50% T_N	100% T_N
	Motor speed	10% n_N	50% n_N	75% n_N	100% n_N
	Control modes	Vector control	V/f control	-	-
Voltage sag characteristics	Sag types	Type I	Type II	Type III	
	Voltage magnitude before voltage sag	90% U_N	110% U_N	-	
	Harmonics	THD= 5%	THD= 10%	-	

Note: T_N is rated motor torque, n_N is rated motor speed, and U_N is nominal voltage of power source.

During the test, a computer controls the voltage sag source to obtain voltage sags and short interruptions. The state of PMSM is recorded to judge whether the VFDs can tolerate a disturbance. The voltage sag magnitude or duration is changed to obtain the critical tolerance of the tested VFDs by successive approximation method. Thus, the data used to determine a voltage sag tolerance curve of certain equipment is attained. The tolerance curve is constructed by analyzing and processing the data.

IV. TEST RESULTS AND ANALYSIS

A. INFLUENCE OF LOAD TORQUE AND SPEED

Voltage sag tolerance curves of VFDs under different motor torque are obtained after processing of the test data. And taking the test results of VFD_1 and VFD_5 as examples, the voltage sag tolerance curves of them are shown respectively in Fig. 4 (a) and Fig. 4 (b). Judging from Fig. 4, as the motor torque is increasing from 0% to the rated torque, the critical duration of VFD voltage sag tolerance curve is decreasing with the larger magnitude range, and the critical voltage magnitude has a tendency to increase with the smaller magnitude range and fluctuates around 70% of rated voltage magnitude. Therefore, the larger the motor torque is, the weaker the voltage sag tolerance capability of VFDs is, which is consistent with the mechanism analysis.

Voltage sag tolerance curves of VFDs under different motor speeds are obtained after processing of test data. And taking the test results of VFD_1 and VFD_5 as examples, the voltage sag tolerance curves of them are shown respectively in Fig. 5 (a) and Fig. 5 (b). In theory, the faster the motor speed is, the larger the load power is, and the weaker the voltage sag tolerance capability of VFDs is. And it can be seen from the test results that the critical duration decreases while critical voltage magnitude increases for VFD_1 with the increase of the motor speed, which is consistent with the mechanism analysis, but the tolerance curves of 75% n_N and 50% n_N are overlapping. And the test results of VFD_5 show

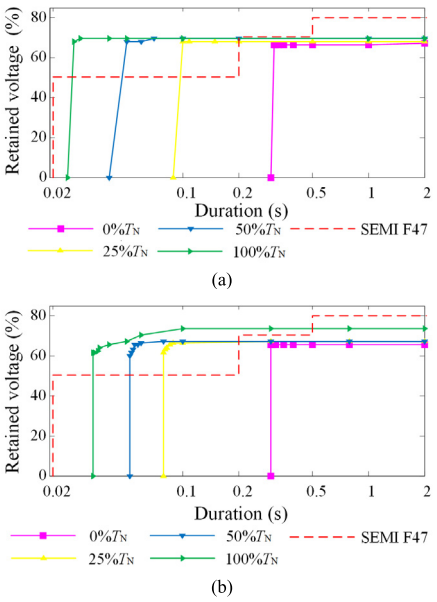

FIGURE 4. VTCs under various torque with rated speed. (a) VFD_1. (b) VFD_5.

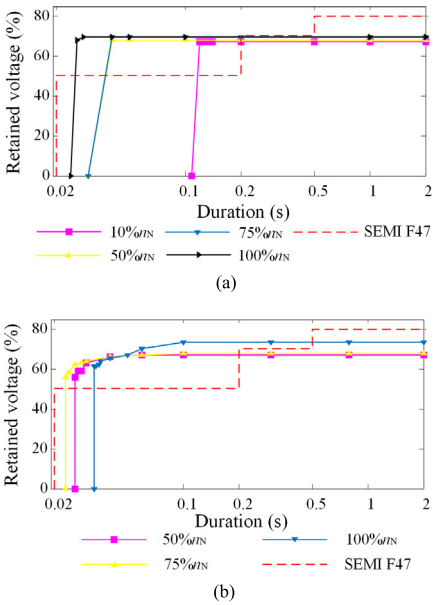

FIGURE 5. VTCs under various speed with rated torque. (a) VFD_1. (b) VFD_5.

that the critical voltage magnitude increases with the increase of the motor speed, but the critical duration does not strictly consistent with the relationship with motor speed: the critical duration of 75% n_N and 50% n_N is longer than that of 100% n_N. This is related to the control performance of the VFD. The control performance of VFDs is more stable and the output PWM waveform is more integrated at rated motor speed so that it is less susceptible to the fluctuation of the power supply voltage comparing with VFDs at the lower motor speed [6].

Fig. 6 shows the Type III voltage sag tolerance curves of the 8 VFDs at rated speed and torque, from which we can see that

the critical duration that the 8 VDFs can tolerate is ranging from 12 ms to 62 ms, and the critical voltage magnitude is ranging from 64% to 73%; different VFDs have obviously different tolerance curves, while VFDs in different power do not show apparent difference in tolerance curves.

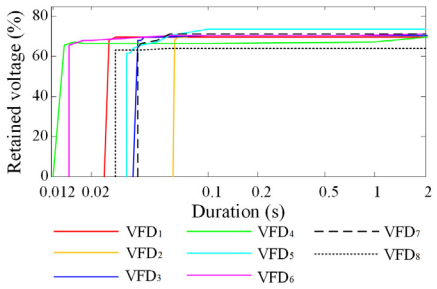

FIGURE 6. VTCs of 8 VFDs under rated status for Type III.

B. INFLUENCE OF VOLTAGE SAG TYPES

The obtained tolerance curves of Type I, Type II, and Type III voltage sags are shown in Fig. 7 with rated motor torque and speed and vector control mode. From Fig. 7(a), we can see that the tolerance curve of VFD_5 on Type III voltage sags has the maximum fault area with the minimum critical duration and the maximum critical voltage magnitude; the tolerance curve of VFD_5 on Type I voltage sags has the minimum fault area with the maximum critical duration and the minimum critical voltage magnitude; the tolerance curve of VFD_5 on Type II voltage sags has critical voltage magnitude of 50%, while it does not have critical duration. From Fig. 7 (b), we can see that the tolerance curve of VFD_3 for Type III voltage sags has the maximum fault area and the tolerance curve of VFD_3 on Type II has the minimum critical voltage magnitude, and VFD_3 is immune to the Type I voltage sags so that there is no tolerance curve of VFD_3 on Type I. In conclusion, the tolerance capability of VFDs for Type I, Type II, and Type III voltage sags decreases in turn, which is consistent with the mechanism analysis.

Particularly, the tolerance curve of VFD_2 shown in Fig. 7 indicates that the VFD is more sensitive to Type I voltage sag than Type II, which is different with the mechanism analysis. It is found that Type II and Type I voltage sags will not trigger low-voltage protection or over-current protection in VFD_2 and there is another protection mode open-phase protection in VFD_2 except the protections mentioned above during the tests. Open-phase protection makes VFDs trip if there is one of the phases whose voltage is less than a certain threshold. The severest Type II voltage sag is set to be 50% voltage magnitude and 1 min duration [16], which does not exceed the threshold, so VFD_2 is immune to Type II voltage sag. Table 4 shows the immunity capability of 8 VFDs on Type II and Type I voltage sags.

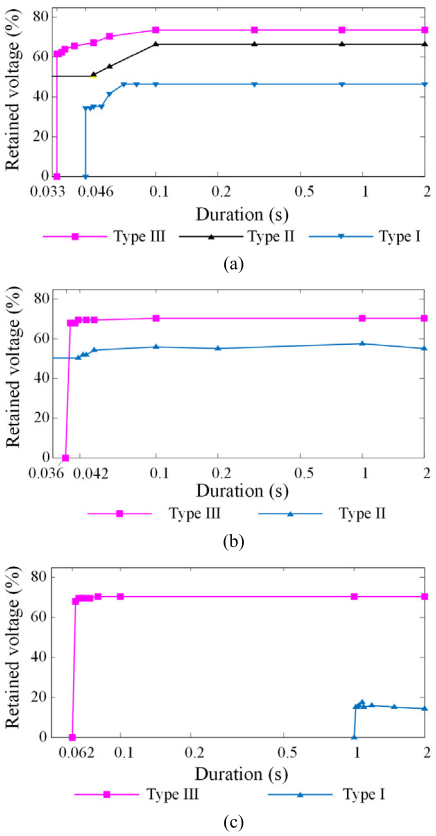

FIGURE 7. VTCs under different sag types. (a) VFD_5. (b) VFD_3. (c) VFD_2.

TABLE 4. Immunity capability of VFDs on Type II and Type I voltage sags.

VFD	Immune to Type I sag,yes (√) or no (×)	Immune to Type II sag,yes (√) or no (×)	One-phase protection,yes (√) or no (×)
VFD_1	√	√	√
VFD_2	×	√	√
VFD_3	√	×	√
VFD_4	×	×	√
VFD_5	×	×	√
VFD_6	×	×	√
VFD_7	√	√	√
VFD_8	×	×	√

C. INFLUENCE OF CONTORL MODES

The default control mode of these 8 VFDs is vector control. Fig. 8 shows the tolerance curves of VFD_1 under V/f control and vector control, the voltage sag type kept Type III and the motor torque and speed kept rated during the tests. When the motor torque and speed are both rated, VFDs under V/f control mode is a little bit more sensitive than they under vector control mode, because vector control mode improves the stability of control on VFDs and makes VFDs stronger immunity ability.

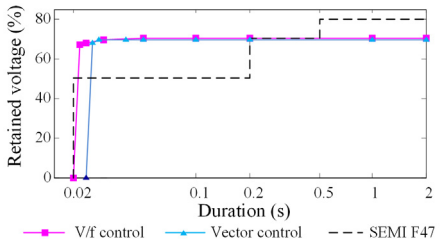

FIGURE 8. VTCs under different control strategy.

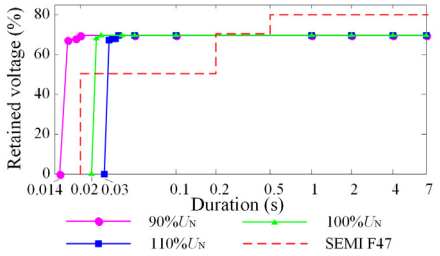

FIGURE 9. VTCs under different pre-sag voltage.

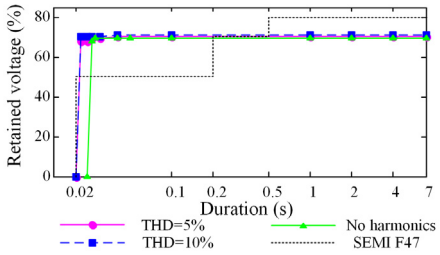

FIGURE 10. VTCs under combined harmonic orders.

D. INFLUENCE OF VOLTAGE MAGNITUDE BEFORE VOLTAGE SAG

The tolerance curves under different voltage magnitudes before voltage sags have been obtained after analyzing and processing the test data, and the tolerance curve of VFD_1 is shown in Fig. 9. It is shown that the voltage magnitude before voltage sag mainly affects the critical duration, and the smaller the voltage magnitude on AC side before voltage sag is, the smaller the voltage on DC bus is, so the critical duration of VFDs' tolerance curve is smaller.

E. INFLUENCE OF HARMONICS

The tolerance curves of VFDs under the combination of 3rd, 5th and 7th harmonics are shown in Fig. 10. It can be seen that the tolerance capability decreases slightly as the total harmonic distortion increases from 5% to 10%.

F. GENERAL TOLERANCE CURVE OF LOW-VOLTAGE VFDs

A large number of tolerance curves were extracted through plenty of repetitive tests on the 8 VFDs. And envelop these tolerance curves respectively for different types of voltage sags by processing about 13000 test data under rated torque and rated speed. First, the maximum and minimum values of withstanding duration under a certain voltage magnitude are selected, and then the maximum and minimum withstanding duration are connected to obtain the envelope of the tolerance curves. Considering that VFDs usually operate at rated torque and speed in actual application, tolerance curves of VFDs extracted on different types of voltage sags are all on the rated working conditions.

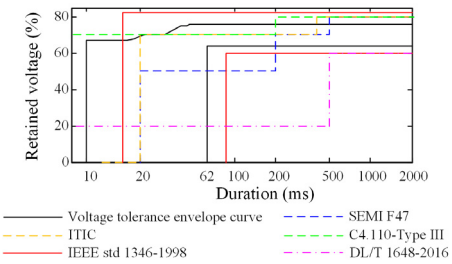

FIGURE 11. Universal VTCs under Type III sags.

1) THE GENERAL TOLERANCE CURVE OF VFDS ON TYPE III VOLTAGE SAGS

When Type III voltage sags occur, the tolerance curve of VFDs has two envelopes and a region where the state of the VFDs between them is uncertain. The critical duration is from 10 ms to 62 ms, and the critical voltage magnitude is from 64% to 76%. These tolerance curves obtained from the current tests are compared with the ITIC, SEMI, and C4.110 curves. However, the shapes of these curves do not match exactly with one other. Compared with the critical duration and critical voltage magnitude of VFDs specified in IEEE Std 1346-1998 in 1998. Differences were found in the critical ranges obtained from the voltage sag tolerance tests of the eight VFDs in this study. Critical voltage and critical duration magnitudes of the upper envelope decreased by 6% and 23 ms, respectively. Thus, the current ability of the most sensitive VFDs to withstand voltage magnitude is improved but their ability to withstand voltage sag duration is diminished. Critical voltage magnitude and critical duration of the lower envelope increased by 4% and 8 ms, respectively. Therefore, the immunity ability of current VFDs that are the least sensitive to voltage sag is diminished. Overall, the voltage sag tolerance capability of current VFDs is not consistent with the standards mentioned. This general tolerance curve obtained in these repetitive tests may provide an important reference for the development of Type III voltage sag tolerance standards for low-voltage VFDs.

2) THE GENERAL TOLERANCE CURVE OF VFDS ON TYPE I AND TYPE II VOLTAGE SAGS

Fig. 12 shows that the tolerance characteristic of VFDs on Type II voltage sags is approximately a horizontal curve, and the sag magnitude fluctuates between 50% and 66%; whereas the tolerance characteristic of the VFDs on Type I voltage

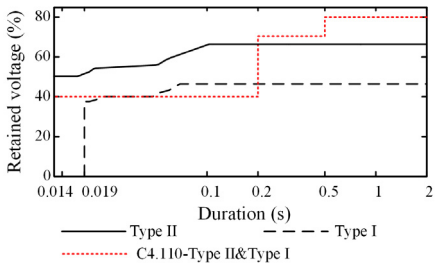

FIGURE 12. The general tolerance curve of VFDs on Type I and Type II sags.

sags is approximately rectangular, and the critical value of duration is 19 ms and the voltage threshold fluctuates between 37% and 46%. The tolerance curves for Type I and Type II sags proposed by C4.110 are not consistent with the tolerance characteristics of tested VFDs. The general tolerance curve obtained from the test can provide an important reference for the development of relevant standards.

Unlike Type III voltage sags, some VFDs are immune to Type I and Type II voltage sags, and their tolerance curves cannot be drawn on the VT plane. Therefore, VFDs only have an upper envelope for tolerance curve of Type I and Type II voltage sags. It divides the VT plane into two areas. The area above and below the envelope are the normal and uncertain areas, respectively.

The general tolerance curves of the VFDs for different sag types under the rated torque speed is shown in Fig. 13, which offer important references to develop the VFDs' tolerance curve standard, improve the performance of VFDs, and promote the voltage sag management.

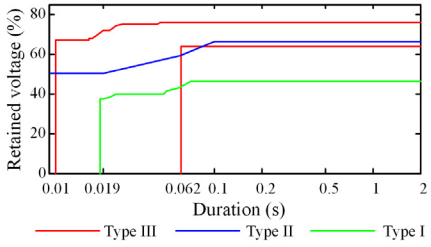

FIGURE 13. The general tolerance curve of VFDs on different types of sags.

V. INFLUENCE OF VOLTAGE SAG ON THE OPERATION PERFORMANCE OF PMSM

As the load in the tests on voltage sag tolerance characteristics of VFDs, PMSM will lose synchronous speed in a short time even if the VFD can withstand voltage sag, and its performance differs obviously when driven by different VFDs. Therefore, this section first analyzes the mechanism of the effect of voltage sag on a PMSM, and then studies the influence of voltage sag on the operating characteristics of the motor based on the data obtained from the voltage sag tolerance tests.

A. THE INFLUENCE MECHANISM OF VOLTAGE SAG ON THE PERFORMANCE OF PMSM

The simplified mathematical model of PMSM is shown as (13), and its electromagnetic torque equation and mechanical movement equation can be shown as (14) and (15) [18].

$$\begin{cases} U_{\mathrm{d}} = (R_{\mathrm{s}} + pL_{\mathrm{d}})i_{\mathrm{d}} - \omega_{\mathrm{r}} L_{\mathrm{q}} i_{\mathrm{q}} \\ U_{\mathrm{q}} = (R_{\mathrm{s}} + pL_{\mathrm{q}})i_{\mathrm{q}} + \omega_{\mathrm{r}} L_{\mathrm{d}} i_{\mathrm{q}} + \omega_{\mathrm{r}} \psi_{\mathrm{f}} \end{cases} \tag{13}$$

$$T_{\mathrm{e}} = P(\psi_{\mathrm{d}} i_{\mathrm{q}} - \psi_{\mathrm{q}} i_{\mathrm{d}}) = P[\psi_{\mathrm{f}} i_{\mathrm{q}} + (L_{\mathrm{d}} - L_{\mathrm{q}}) i_{\mathrm{d}} i_{\mathrm{q}}] \tag{14}$$

$$J\frac{d\omega_{\mathrm{r}}}{dt} = P(T_{\mathrm{e}} - T_{\mathrm{L}} - B\frac{\omega_{\mathrm{r}}}{P}) \tag{15}$$

where U_{d} and U_{q} represent the voltage on d- and q-axes, respectively; i_{d} and i_{q} represent the current on d- and q-axes; L_{d} and L_{q} are the inductance on d- and q-axes; ψ_{d} and ψ_{q} are the magnetic flux on d- and q-axes; p is integral operator; R_{s} is the resistance of the armature winding; P is the number of rotor pole pairs; T_{s} and T_{L} represent the electromagnetic and load torque; J is the rotary inertia of the rotor and B is the damping coefficient.

For the PMSM driven by a VFD, the VFD is first affected when a voltage sag event occurs. If protections of VFD are not triggered when the voltage on the DC side has been the minimum, the output voltage of the VFD, which supplies the motor and is equal to phase voltage of motor stator, will be lower than the rated voltage. Thus, the PMSM will operate in a low-voltage state. According to (13) to (15), when the motor input voltage u_{d} and u_{q} decrease, i_{d} and i_{q} will decrease, thereby resulting in a decrease in electromagnetic torque and an imbalance between electromagnetic and load torques. However, the mechanical response speed is much smaller than the electromagnetic response speed. Thus, motor speed does not change immediately. Generally, motor speed decreases after a few seconds. When the voltages on the DC and AC sides of the VFD are balanced, the voltage on DC side stops decreasing. The stator current magnitude, electromagnetic torque, and motor speed exhibit a slight step phenomenon, and then return to normal and finally enter a balanced stage due to the PI control of PMSM [19]. At the end of the voltage sag, the recover balance between DC side voltage and the supply voltage is broken again. The duration of this process is almost negligible, whereby the stator current suddenly increases due to the steep increase of the stator phase voltage, which contributes to the increment of the electromagnetic torque and motor speed. Then, PMSM recovers to normal operation after a brief control period. If the duration is extremely short, then no equilibrium stage may exist. Therefore, the duration of the sag also affects the variation of the motor speed and stator current throughout the process.

B. TEST DATA STUDY ON INFLUENCE OF VOLTAGE SAGS ON PMSM

The most important difference among VFDs is how they are controlled, which lead to the varied performance of PMSM. So the waveform of VFD_1 on V/f control mode and vector

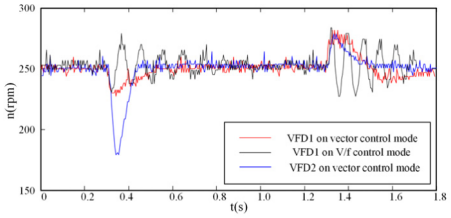

FIGURE 14. Speed waveforms of PMSM.

mode and waveform of VFD_2 on V/f control mode are used in this section to analyze the influence of voltage sags on PMSM. It is found that PMSM is driven by VFD_1 and VFD_2 can withstand voltage sags with duration of 0.02 s and 0.034 s respectively, and will not stop when the voltage magnitude is larger than 70% U_N.

1) THE INFLUENCE OF DIFFERENT VFDS ON MOTOR SPEED

The waveforms of the motor speed under the driving of VFDs is shown in Fig. 14, and the corresponding sag magnitude is 71% and the duration is 1 s.

It can be seen from Fig. 14 that: *a*) After the sag occurs, the motor speeds driving by the different VFDs change significantly, and the change process is basically the same, including speed reduction or vibration, recovery, and smoothing process, and the motor speed would accelerate abruptly and gradually recover at the end of the sag; *b*) There is a difference in the decline depth of motor speed in the conditions of different VFDs on the same control mode and the same VFD on different control modes during the voltage sag. The motor speed suffered the biggest decrease under VFD_1 on vector control mode, the motor speed decreases most slightly under VFD_2 on vector control mode, and the motor speed under VFD_1 on V/f control mode experienced oscillation. *c*) The recovery duration of PMSM driven by different VDFs is obviously different. The recovery time of PMSM under VFD_2 on vector control mode is the shortest, only about 0.15s, while it is the longest, about 0.6 s, for VFD_1 on V/f control mode; *d*) After the voltage sag ends, there is a difference in the increase of the motor speed under different VFDs. The motor speeds both increase at first and then recover under VFD_1 and VFD_2 on vector control mode, while the motor speed significantly vibrates under the driving of VFD_1 on V/f control mode. Besides, the recovery process on vector control mode is shorter with slight fluctuation, and that on V/f control mode is longer with oscillation.

2) THE INFLUENCE OF DIFFERENT VFDS ON STATOR CURRENT

The waveforms of the A-phase stator current of the motor driven by different VFDs during the sag is shown in Fig. 15. The corresponding retained voltage is 71% and the duration is 1 s.

It can be seen from Fig. 15 that the change process of the stator current is similar to that of the motor speed, and the

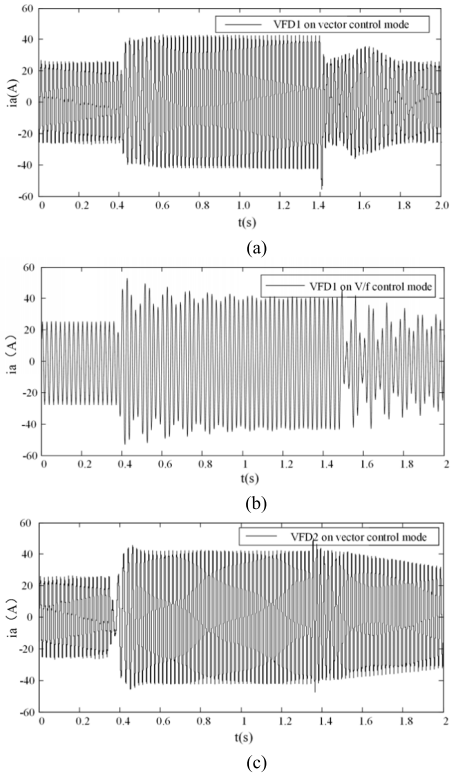

FIGURE 15. Waveforms of stator current. (a) VFD_1 on vector control mode. (b) VFD_1 on V/f control mode. (c) VFD_2 on vector control mode.

waveforms of the motor current of the VFD on vector control mode and V/f control mode are different with each other.

For the motor driven by VFDs on vector control mode, the stator current first enters the declining process when a voltage sag occurs, and its duration is extremely short. Then a step-rise is observed in the stator current, whose duration of VFD_2 is shorter than VFD_1. Thereafter, the stator current undergoes a process in which the stator current becomes stable and is likely more than 50% of the rated current. When the voltage sag is over, the stator current has a transient surge.

For the motor driven by VFD_1 on V/f control mode, the change stage is basically consistent with that of the motor driven by VFDs on vector control mode. However, the increase and decrease on vector control mode becomes an oscillation with longer recovery duration on V/f control mode.

VI. CONCLUSION

This study analyzes the mechanism and phenomenon of VFDs influenced by voltage sags. Based on test results, general tolerance curves for Type I, Type II, and Type III voltage sags are obtained. The characteristics of PMSM affected by voltage sags under different VFDs are determined through the further mechanism and test data analyses. The following specific conclusions are drawn:

Load torque and speed and voltage sag types are important factors that have remarkable influence on the sag tolerance

of VFDs. For voltage sag types, this paper deeply analyzes the influence on the tolerance capability in terms of energy. And the results show that some VFDs have weaker tolerance capability to Type I sags than Type II sags. Type I and Type II sags do not trigger low-voltage and over-current protection, whereas Type I sags triggers an open-phase protection. Other factors have a minimal effect on the VFDs under voltage sags.

After comprehensive analyses and processing of more than 13,000 sets of test data, the general tolerance curves of the low-voltage VFDs for the various types of voltage sags are extracted, and the sag tolerance characteristics of VFDs under actual conditions are revivified. The general tolerance curves have strong representativeness and can provide the basis for the voltage sag tolerance analysis and the voltage sag mitigation measures of VFDs.

Voltage sags cause PMSM driven by VFDs to lose synchronous speed for a short time and cause the stator current to undergo a process similar to that of motor speed. The influence of same VFD varies with different control modes on the operation performance of PMSM, and the influence of different VFDs also varies with same control mode on the operation performance of PMSM. Therefore, considering the characteristics of VFDs and PMSM is necessary in selecting the appropriate combination in engineering.

ACKNOWLEDGMENT

The authors gratefully acknowledge the contributions of Yunbo Long and Wu Yapen for their work on providing testing facilities, feasible ideas and original documents.

REFERENCES

[1] Z. Daojun, "The analysis of frequency converter prevent low voltage ride through," *Jiangsu Elect. Eng.*, vol. 34, no. 2, pp. 37–40, 2015.
[2] X. Liang and J. Hofman, "Trip curves and ride-through evaluation for power electronic devices in power system dynamic studies," *IEEE Trans. Ind. Appl.*, vol. 52, no. 2, pp. 1290–1296, Mar./Apr. 2016.
[3] A. dos Santos and M. T. C. de Barros, "Predicting equipment outages due to voltage sags," *IEEE Trans. Power Del.*, vol. 31, no. 4, pp. 1683–1691, Aug. 2016.
[4] L. E. Weldemariam, H. J. Gärtner, V. Cuk, J. F. G. Cobben, and W. L. Kling, "The performance of sensitive equipment to voltage dips from field measurements," in *Proc. AFRICON*. Addis Ababa, Ethiopia, 2015, pp. 1–5.
[5] S. Z. Djokic, J. V. Milanovic, J. Desmet, K. Stockman, and G. Vanalme, "Influence of voltage sags on personal computers and PWM drives," *Electronics*, vol. 7, no. 2, pp. 110–113, 2003.
[6] M. H. J. Bollen, *Understanding Power Quality Problems: Voltage Sags and Interruptions*. Piscataway, NJ, USA: IEEE Press, 1999.
[7] S. Z. Djokic, K. Stockman, J. V. Milanovic, J. J. M. Desmet, and R. Belmans, "Sensitivity of AC adjustable speed drives to voltage sags and short interruptions," *IEEE Trans. Power Del.*, vol. 20, no. 1, pp. 494–505, Jan. 2005.
[8] P. Angers and F. Lévesque, "Voltage dip immunity of PWM drives with ride-through capabilities," in *Proc. 19th Int. Conf. Elect. Mach. (ICEM)*, Rome, Italy, 2010, pp. 1–5.
[9] L. E. Weldemariam, H. J. Gärtner, V. Cuk, J. F. G. Cobben, and W. L. Kling, "Experimental investigation on the sensitivity of an industrial process to voltage dips," in *Proc. IEEE Eindhoven PowerTech*, Eindhoven, The Netherlands, Jun./Jul. 2015, pp. 1–6.
[10] M. Bollen *et al.*, "Voltage dip immunity of equipment and installations," CIGRE, London, U.K., Tech. Rep. C4.110, Apr. 2010.
[11] *IEEE Recommended Practice for Evaluating Electric Power System Compatibility With Electronic Process Equipment*, Standard 1346-1998, 1998.
[12] R. T. Ugale, Y. BalaKrishna, and B. N. Chaudhari, "Effects of short power interruptions and voltage sags on the performance of line start permanent magnet synchronous motor," in *Proc. 4th IET Int. Conf. Power Electron., Machines Drives*, York, U.K., 2008, pp. 184–188.
[13] F. Huo, W. Li, L. Wang, Y. Zhang, C. Guan, and Y. Li, "Numerical calculation and analysis of three-dimensional transient electromagnetic field in the end region of large water–hydrogen–hydrogen cooled turbogenerator," *IEEE Trans. Ind. Electron.*, vol. 61, no. 1, pp. 188–195, Jan. 2014.
[14] S. Z. Djokic, S. M. Munshi, and C. E. Cresswell, "The influence of overcurrent and undervoltage protection settings on ASD sensitivity to voltage sags and short interruptions," in *Proc. 4th IET Conf. Power Electron., Machines Drives*, York, U.K., 2008, pp. 130–134.
[15] C. Cong, *Study on Test Method on Sensitivity of AC Adjustable Speed Drives to Voltage Sags*. Beijing, China: North China Electric Power Univ., 2017.
[16] *IEEE Standard Association. IEEE Trial-Use Recommended Practice for Voltage Sag and Short Interruption Ride-Through Testing for End-Use Electrical Equipment Rated Less Than 1000V*, Standard P1668-2014, 2014.
[17] *IEEE Recommended Practice and Requirements for Harmonic Control in Electric Power Systems*, Standard 519-2014, IEEE Applications Society/Power Engineering, 2015.
[18] L. Jilong, X. Fei, S. Yang, M. Zhiqin, and L. Chaoran, "Position-sensorless control technology of permanent-magnet synchronous motor—A review," *Trans. China Electrotech. Soc.*, vol. 32, no. 16, pp. 76–88, 2017.
[19] Q.-B. Hu and C.-Y. Sun, "Sensorless control of permanent magnet synchronous motor in full speed range," *Electr. Mach. Control*, vol. 20, no. 9, pp. 73–79, 2016.

YONGHAI XU was born in Xinye, Henan, China, in 1966. He received the B.S. degree from Tsinghua University, and the M.S. and Ph.D. degrees from North China Electric Power University, Beijing, China.

He is currently a Professor with the School of Electrical and Electronic Engineering, North China Electric Power University. His research interests include power quality analysis and control, and new energy power system.

WENQING LU was born in Fuzhou, Fujian, China, in 1994. She received the B.S. degree in smart grid information engineering from North China Electric Power University, where she is currently pursuing the M.S. degree. Her research interests include power quality and its control.

KUN WANG was born in Anqing, Anhui, China, in 1994. He received the B.S. degree in smart grid information engineering from North China Electric Power University, where he is currently pursuing the M.M. degree. His research interests include power quality and its control.

CHENYI LI was born in Neijiang, Sichuan, China, in 1994. She received the B.S. degree in power system and automation from Xiamen University, and the M.S. degree in power system and automation from North China Electric Power University.

She is currently with State Grid Chengdu Power Supply Company. Her research interest includes power quality.

WASEEM ASLAM was born in Muzaffargarh, Punjab, Pakistan. He received the B.S. degree in electrical engineering (power) from UCET, in 2011, and the M.S. degree in electrical engineering (power) from the Islamia University of Bahawalpur, Punjab, Pakistan, in 2013.

He is currently pursuing the Ph.D. degree with North China Electric Power University, Beijing, China. He was an Electrical Engineer with the Government Engineering Institute. His research interests include power quality improvement, power system stability, and smart grids.